STUDIES OF REACTION GEOMETRY IN OXIDATION AND REDUCTION OF THE ALKALINE SILVER ELECTRODE

FIFTH QUARTERLY REPORT

Eliot A. Butler

Angus U. Blackham

August 15, 1969

J. P. L. 952268

Brigham Young University

Provo, Utah

STUDIES OF REACTION GEOMETRY IN OXIDATION AND REDUCTION OF THE ALKALINE SILVER ELECTRODE

FIFTH QUARTERLY REPORT

Eliot A. Butler

Angus U. Blackham

August 15, 1969

J. P. L. 952268

This work was performed for the Jet Propulsion Laboratory, California Institute of Technology, as sponsored by the National Aeronautics and Space Administration under Contract NAS7-100.

Brigham Young University

Provo, Utah

This report contains information prepared by Brigham Young University under JLP sub-contract. Its content is not necessarily endorsed by the Jet Propulsion Laboratory, California Institute of Technology, or the National Aeronautics and Space Administration.

ABSTRACT

In c.c.s. (cyclic current step) measurements improved electrode reproducibility has yielded data sufficiently accurate to confirm the non-linearity of the plot of exchange current density versus time of oxidation. The interruption of the d.c. charging current in order to make c.c.s. measurements causes increased length of the first plateau, distortion in the wave form of the voltage response, and instability of those responses during the first few minutes after the interruption. These observations indicate that a physical change of the electrode occurs during the a.c. cycling. As electrolyte contaminants, O_2 and CO_2 have been shown to affect measurements of electrode resistance and of charging plateau length by as much as 25%.

The charge acceptance by silver foil electrodes under potentiostatic conditions in alkaline solution has been measured by current-time integral, constant current reduction, and atomic absorption techniques. All measurements show the same charge acceptance versus potential relationship, thus indicating that the large maxima and minima in the charge acceptance are real. Results from potential sweep oxidations suggest the formation of two types of silver(I) oxide. This fits in with the proposal of others[9] that the initial silver(I) oxide is a thin layer of randomly oriented crystallites.

Model pore electrodes of several pore sizes were constructed and have demonstrated that a decrease in pore size is accompanied by a shorter penetration of oxide into the pore. Penetration is also shortened by increased velocity of electrolyte flow. The reaction current density was approximately the same for oxidations of equal plateau

length, regardless of pore size. The design of the model pore electrode shows considerable promise in the investigation of reactions in the confines of a pore, an area which has received much theoretical attention.

TABLE OF CONTENTS

S E C T I O N I

KINETIC STUDIES OF THE OXIDATION OF SILVER IN ALKALINE ELECTROLYTE

Introduction

Cyclic current step (c.c.s.) measurements on partially oxidized silver electrodes in alkaline solution have been previously reported.[1] The rapid drop in the double layer capacitance as oxide forms on the electrode makes the method feasible for this system, while it could not be used on the unoxidized electrode in alkaline solution because of the high capacitance. The shape of the $\Delta\eta_\theta$ versus $1/\sqrt{f}$ curves obtained at various points on the Ag-Ag_2O plateau is very similar in shape to those from systems in which the method directly applies (i.e. ferrous-ferric system[2]). Exchange current density, "i_o", values calculated from c.c.s. measurements were shown to decrease in magnitude with increased time of oxidation. However, complications arising from differences in mechanism of reaction between an electrode that forms an oxide layer and an inert electrode may not justify direct application of the method. Further investigations and results of the use of the method are reported here.

Two common contaminants of KOH electrolyte are O_2 and $CO_3^=$. The effect of these impurities on the behavior of the Ag electrode during various measurements has not been thoroughly investigated. The $CO_3^=$ is particularly suspect because of the high solubility of CO_2 in alkaline solutions and because of the varying amounts of CO_2 found in the air exposed to the electrolyte at different times. The effect of these two impurities will be discussed briefly in this report.

Experimental

An additional change has been made in the apparatus we were using for c.c.s. measurements previously reported.[1] The circuit for the apparatus currently in use is shown in Figure 1. The change was the removal of the resistance loop which was connected in parallel with the test cell. This loop was part of a bridge circuit used to balance out the ohmic voltage response of the cell. It was found, however, that with the solution concentration with which we are working, the ohmic component of the voltage response is negligibly small. A third electrode is used instead of the counter electrode as the reference electrode. This eliminates the inaccuracies associated with the slight polarization of the counter electrode.

The c.c.s. measurements were made at various points along the $Ag\text{-}Ag_2O$ plateau during the oxidation of the silver electrode in 1.04 F KOH. The temperature for the measurements was $25 \pm 0.1^{o}C$. The square wave current density was 0.412 ma/cm^2. The points along the potential-time curve where c.c.s. measurements were made and i_o values determined are shown in Figure 2. The c.c.s. measurements were made by interrupting the direct current oxidation, balancing the e.m.f. of the test cell with a voltage divider so that less than 1 μamp of current was flowing and then, as previously described[3], observing the magnitudes of the peak-to-peak electrode voltage, $\Delta\eta_\theta$ at several frequencies of the square wave current. Values of i_o were calculated from the intercept obtained by extrapolating to infinite frequency the linear portion of a plot of $\Delta\eta_\theta$ versus $1/\sqrt{f}$. Plots of this type have been previously reported.[1] For the data reported here, only one interruption was made in the d.c. oxidation of each electrode.

Fig. 1

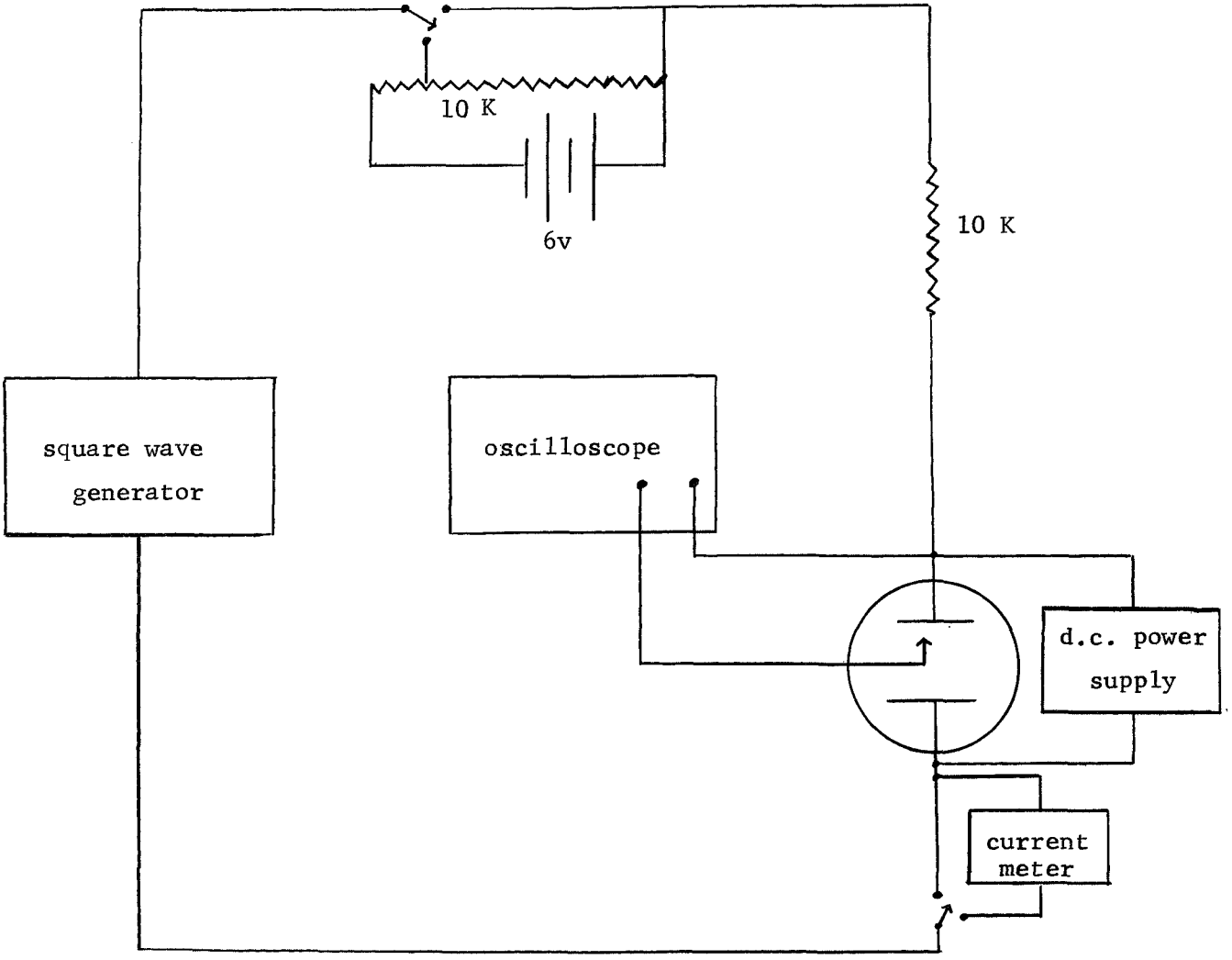

Fig. 1 -- Modified c.c.s. circuit diagram.

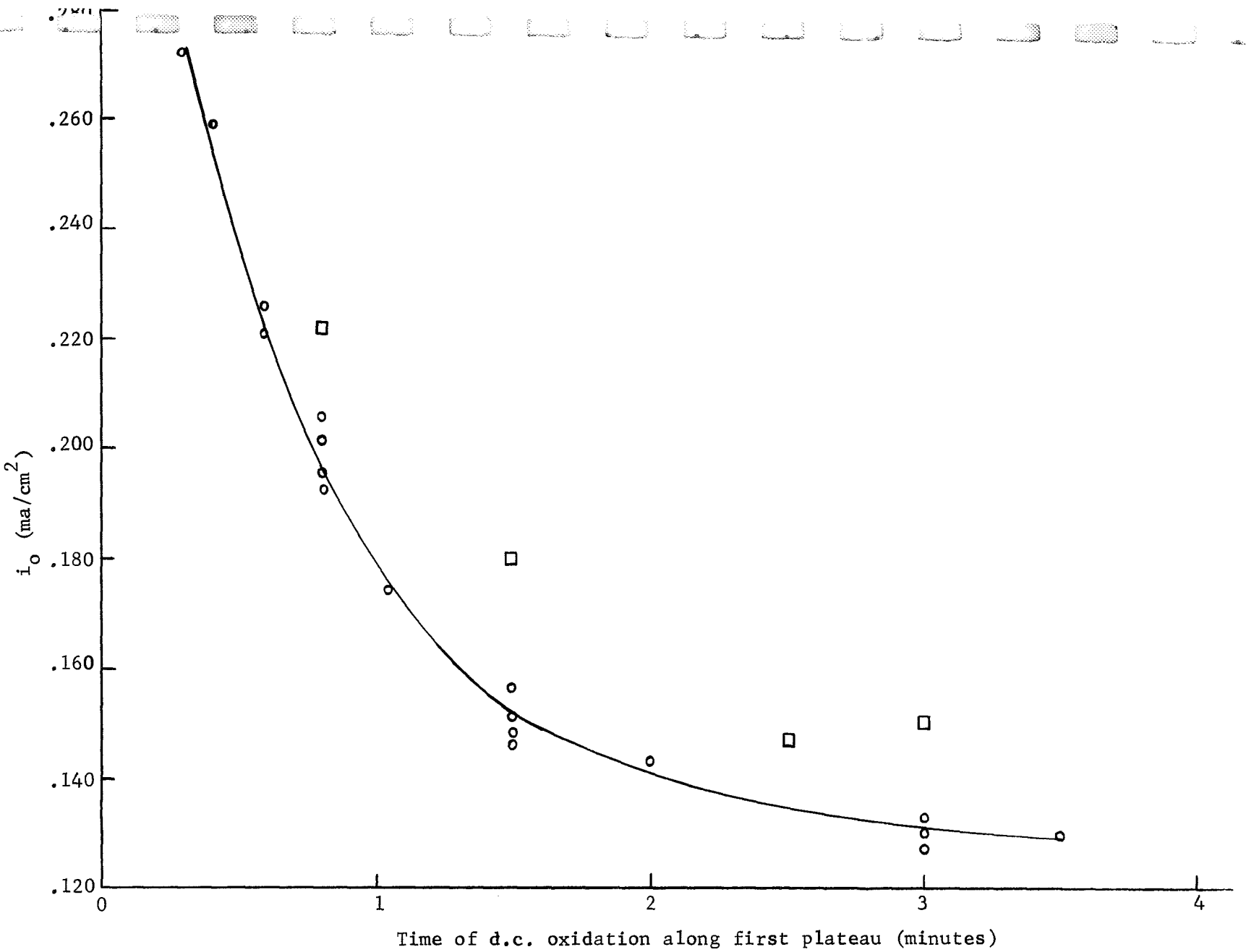

Fig. 2 -- Plot of i_o versus time of oxidation along first plateau. Square wave current density 0.412 ma/cm^2. Total first plateau length ~ 4.0 minutes. ◘ = points calculated from c.c.s. measurements taken before oscilloscope trace had stabilized. o = points calculated after stabilization.

This helped minimize the problem of increase in total charge acceptance during the Ag-Ag_2O plateau due to repeated interruption of the d.c. oxidation.

Because only one i_o determination was made during each oxidation, the problem of reproducibility of the first oxidation plateau had to be dealt with. The following procedure was used for preparation of the electrodes. Silver wire (26 gauge) was cut into proper lengths for the electrode, wiped with absorbent paper, and dipped in alcoholic KOH. The electrode was then rinsed thoroughly in distilled water, and anodized in ammonia solution for about four minutes at a current density of 0.4 ma/cm^2. Then the electrode was rinsed and stored in distilled water until it was used. After having been oxidized once in KOH, the electrodes were merely dipped in ammonia solution, rinsed and stored again in the distilled water.

The method and apparatus for measuring oxide film resistance were described in previous reports[1, 4]. To test the effects of impurities on the total charge acceptance and on the maximum resistance, a carbonate-free KOH solution was prepared. This was done by adding sufficient $Ba(OH)_2 \cdot 8H_2O$ to a 1.09 F KOH solution to precipitate all the carbonate as $BaCO_3$. The solution was then filtered and the excess Ba^{++} was removed by addition of K_2SO_4 until no further precipitate formed. The solution was then passed through an ion exchange column of amberlite I R 120, which had been charged with KCl, to remove traces of Ba^{++}. Estimated Ba^{++} contamination was 0.02% and $SO_4^{=}$ contamination was 0.01%. To test for the effect of $CO_3^{=}$ contamination, known amounts of K_2CO_3 reagent were added to the $CO_3^{=}$ free KOH. To test for the effect of O_2 contamination, air was bubbled through the solution, which had previously

been purged with nitrogen. The charge acceptance and maximum resistance in these solutions were compared to runs made in nitrogen purged carbonate-free solutions.

RESULTS AND DISCUSSION

Cyclic Current-Step Measurements

The decrease in the i_o value, calculated from c.c.s. measurements, with increasing depth of oxide during the Ag-Ag_2O oxidation plateau has been previously reported.[1] However, the shape of the curve of i_o vs time of oxidation was believed to be distorted because of the effect of repeated interruptions in the d.c. oxidation. Figure 2 shows recent values in which the effect of these interruptions has been minimized by making only one interruption per oxidation. These values were obtained at a lower square wave current density than those previously reported. Another change was the use of new, unoxidized electrodes rather than electrodes which had been oxidized and reduced several times.

The method of preparation of the electrodes used gives more reproducibility in first plateau lengths and therefore the depth of the oxide film can be controlled merely by controlling time of oxidation. Since the depth of the oxide film appears to be the determining factor in the value of the $\Delta\eta_\theta$ measurements, and i_o values are calculated from the intercept of $\Delta\eta_\theta$ versus $1/\sqrt{f}$ plots, the i_o values are also more reproducible. In the procedure for preparation of electrodes previously used, the electrolytic surface area varied so much that a particular depth of oxide could not be reproduced. Table I shows first plateau length and per cent deviation from the mean in the first plateau for five electrodes. The table shows data for the oxidation after the initial electrode preparation and also after the

TABLE I

Reproducibility of First Oxidation Plateau During First, Second and Third Oxidations After Preparing Electrodes as Outlined in Procedure.

Oxidizing Current Density 0.74 ma/cm^2, Temperature 25°C

Run No	Plateau Length (min)	% Deviation from Mean
	First Oxidation	
1	2.65	0.0 %
2	2.69	1.50%
3	2.64	.38%
4	2.62	1.13%
5	2.67	.75%
	Second Oxidation	
1	2.68	0.0 %
2	2.76	3.5 %
3	2.92	2.1 %
4	2.92	2.1 %
5	2.86	0.0 %
	Third Oxidation	
1	2.62	6.8 %
2	2.70	3.9 %
3	2.78	1.1 %
4	2.86	1.8 %
5	3.10	13.8 %

second and third oxidations. For the second and third oxidations the electrode was prepared by dipping the once used, oxide covered electrode into ammonia solution and rinsing as already explained. It is noted that the reproducibility gets worse with each successive oxidation, probably due to increasing roughness and nonuniformity of the surface.

These changes in experimental conditions had significant effects on the i_o values reported here. The plot of i_o versus time of oxidation shows more curvature than the similar plot previously reported. The dissimilarity between the two curves is probably the result of the different number of interruptions in the d.c. oxidation. Also the magnitude of the i_o values calculated from these data differ by a factor of about 5 (being 1/5 as large) from those previously reported. Differences in the roughness factors of the two sets of electrodes may cause some difference in the magnitude of i_o, since the i_o calculations were based on geometrical surface areas rather than actual electrolytic surface areas. The procedure for the preparation of the electrodes previously used, namely the sanding of the surface and the repeated cycling of the electrode before measurements were made would give electrodes with larger roughness factors than would the procedure reported here which gives much better reproducibility.

The effect of the square wave current is also noted in the difference of the i_o values. Ideally, the same i_o value should be obtained regardless of the square wave current density until at high square wave current densities the voltage response of the electrode is large enough that the relationship of Wijnen and Smit[5] no longer applies. However, this was not found to be the case. At low current densities, <0.19 ma/cm^2, the plot of $\Delta\eta_\theta$ versus $1/\sqrt{f}$ shows no linear region.

This results from the high capacitance of the electrode which the small current density is unable to charge through. At current densities between 0.19 ma/cm^2 and 0.42 ma/cm^2 the i_o values hold quite constant as should be the case if the method is working correctly. Above 0.42 ma/cm^2 several complications arise in making the experimental measurements. The i_o values calculated from the intercept increase with increasing current density. This is shown in Figure 3 which is a plot of i_o versus the square wave current density. At lower frequencies of the high square wave current densities distortion appears in the wave form displayed on the oscilloscope. This wave form is compared to the expected waveform in Figure 4.

The c.c.s. method as developed by Wijnen and Smit[5] was specifically derived for use on a system in which both electroactive species were present in solution, and the reaction was taking place on an inert electrode (i.e. the ferrous-ferric system with a platinum electrode[2]). A further qualification was that the overvoltage be diffusion dependent and obey Fick's second law.

In the case of the Ag-Ag_2O electrode in alkaline solution, one electroactive species involved in the electrochemical reaction is in the electrode itself. Also, the presence of the oxide film complicates the mechanism of reaction. It may be that the overvoltage is no longer sufficiently dependent on diffusion of some species from the bulk solution, but rather diffusion or migration of some species through the oxide layer. The general shape of the plot of $\Delta\eta_\theta$ versus $1/\sqrt{f}$ is very similar to that obtained from the ferrous-ferric system. However, one complication arises here also. The voltage response of the electrode which is 60 to 80 mv, is considerably higher than the approximately

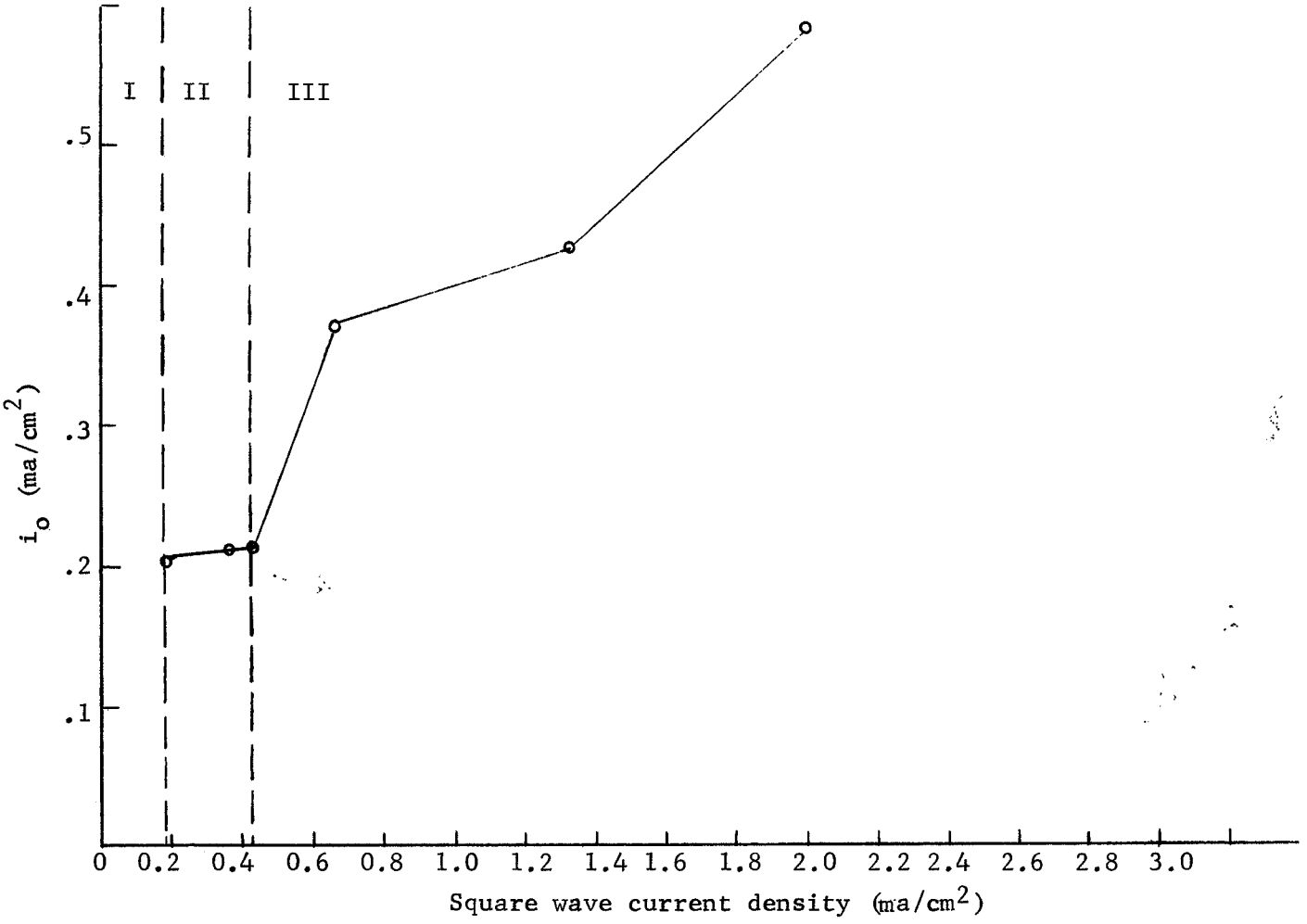

Fig. 3 -- Plot of i_o versus square wave current density at 1 minute into d.c. oxidation. I-region where plots of $\Delta\eta_\theta$ versus $1/\sqrt{f}$ give no linear portion. II-region where i_o is constant with increasing square wave current density. III-region where voltage response is distorted at low frequencies, and i_o increases with increasing current density.

Fig. 4 -- a) normal electrode voltage response. b) distorted electrode voltage response.

10 mv recommended by Wijnen and Smit.[5] This high voltage response of the Ag-Ag_2O electrode is necessary since the square wave current must be sufficient to charge through the high capacitance of the double layer of the Ag-Ag_2O electrode in alkaline solution in order to give a meaningful voltage response.

Another consideration is the effect of the square wave current on the structure and surface properties of the oxide film. It has been reported by Wales[6] that the charging capacity of the alkaline silver electrode can be increased 40-50% by superimposing an a.c. signal on the d.c. oxidizing current. Although in our case the square wave current and the d.c. current are not running simultaneously, the instability of the voltage response after application of a square wave current at a particular frequency indicates surface or structural changes in the oxide. Figure 5 shows plots of voltage response versus time since interruption of the d.c. oxidation for five different frequencies and at 3 different points in the oxidation plateau. Significant features of this plot are: (1) the instability of the voltage response during the first few minutes after the interruption, (2) the relatively parallel lines of stable voltage response at later times, and (3) the fact that the plot made at 3 minutes into the d.c. oxidation took several minutes more to stabilize than was needed at 0.8 minutes or 1.5 minutes into the oxidation. These features lend support to the argument that the electrode is being physically changed by the pulsed current, since according to Wijnen and Smit[5], only about 100 cycles at any frequency should be needed to give a stable voltage response. The curve in Figure 2 was obtained from data in the stable regions of Figure 5.

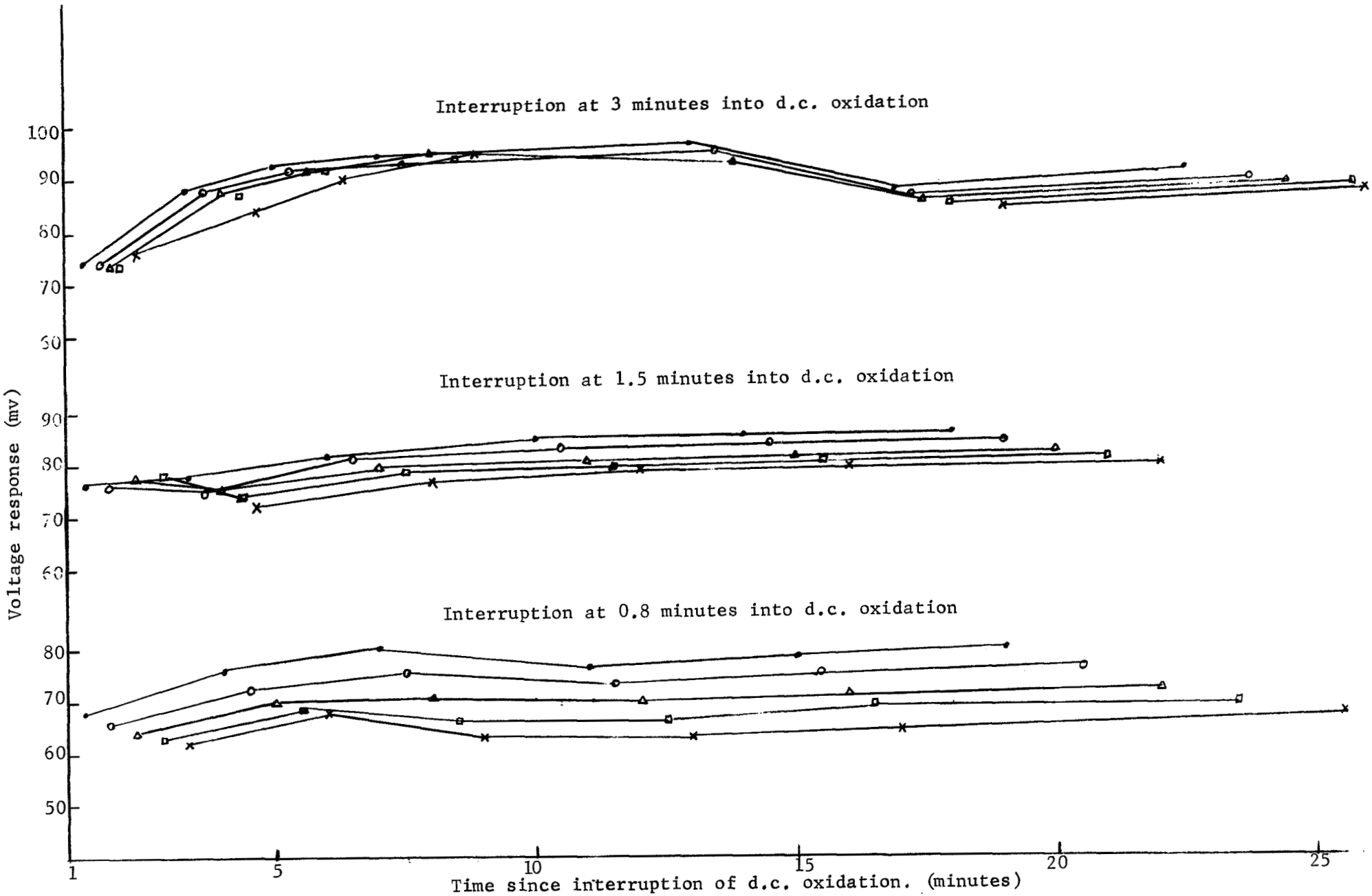

Fig. 5 --Plot of electrode voltage response versus time since interruption of d.c. oxidation for five different frequencies. • = 3 Hz, ○ = 4 Hz, ▲ = 6 Hz, ▫ = 8 Hz, x = 10 Hz. Square wave current density = .412 ma/cm^2. First plateau length ~ 4.0 minutes.

The distortion in the wave form of the voltage response which occurs at high square wave current densities may also be explained in terms of structural change. Because of these changes and the high current density, a second reaction phase (Ag_2O-AgO) may be the cause of distortion. It is noted that the distortion disappears as one increases the frequency of the a.c. This would be expected if a second reaction is taking place, since only during long current pulses would sufficient potential be built up to cause the second reaction. Also, the distortion occurs only on the anodic portion of the cycle.

Another supporting argument for physical changes in the electrode is the fact that the first oxidation plateau is longer if the electrode is interrupted and an a.c. signal is imposed on the electrode. Part of this increase in length may be explained by dissolution or sluffing off of the oxide during the interruption. However, reduction times show that this cannot account for all the increased length. The structure has apparently become less resistive allowing more Ag_2O to form.

Effect of Impurities

Since O_2 and $CO_3^=$ are common contaminants in KOH electrolyte, the effect of these impurities on charge acceptance and maximum oxide film resistance has been determined. The presence of dissolved oxygen (air) in the electrolyte decreases the second plateau charge acceptance and maximum resistance by about 25%. The addition of 2% K_2CO_3 to carbonate-free KOH increases the maximum oxide film resistance by about 17% but the charge acceptance remains the same. It appears that oxygen has an inhibiting effect on the overall reaction while carbonate only affects the nature of the oxide film formed.

SECTION II

CHARGE ACCEPTANCE OF SILVER ELECTRODES UNDER CONDITIONS OF CONTROLLED POTENTIAL

Introduction

This section of the report deals with the potentiostatic oxidation of silver electrodes in alkaline electrolyte. The fundamental importance of the potential in the electrocrystallization of oxides on metal electrodes[7] suggests that potentiostatic oxidations should be of special value in studies of the mechanism of the oxidation of silver electrodes in alkaline solution.

Relatively little work on potentiostatic oxidations of silver in alkaline solution appears in the literature[8,9]. There have been more papers that deal with continuously changing potential and constant or controlled potential oxidations.[10,11,12]

The most complete work to date on the potentiostatic oxidations of silver is by Fleischmann and Thirsk.[9] They studied the topography and growth of silver(I) and silver(II) oxides formed under constant current and potentiostatic conditions using x-ray, electron diffraction, and electron microscopy. They reported two stages of growth for the silver(I) oxide. First, a thin film of randomly oriented crystallites forms on the surface. Second, a more ordered growth occurs from preferred sites on this film. The initial layer represents only about 20 millicoulombs per cm^2 of the total charge acceptance. According to Fleischmann and Thirsk, it is the migration/diffusion of ions through this thin layer that controls the extent of the reaction on the surface. They did not present complete data on the total charge acceptance versus applied potential for silver(I) oxide, but they did for silver(II) oxide.

In the silver(II) oxide region they found a sharp drop-off in total charge acceptance with increasing potential. This is consistent with the results of Malachesky and Jasinski[8].

Malachesky and Jasinski presented data for the total charge acceptance versus applied potential for both silver(I) and silver(II) oxide. The potential range ran from that which would first produce silver(I) oxide to that required to evolve oxygen. The extended abstract of their paper, however, does not include interpretation of their data.

A plot of total charge acceptance versus applied potential over the same potential range used by Malachesky and Jasinski was given in Figure 8 of the fourth quarterly report.[1] It had the same general shape of their plot in the regions of silver(I) and silver(II) oxide formation; however, a third reaction at potentials just below the evolution of oxygen was found to yield a large charge acceptance peak which was not reported by Malachesky and Jasinski.

The work in this quarter has been centered on the determination of the nature of the initial silver(I) oxide film and total charge acceptance relationships in the silver(I) and (II) oxide regions.

EXPERIMENTAL

Potentiostatic Oxidations

The electronic circuitry and cell design used for the potentiostatic oxidations were the same as described in Figure 11 of the second quarterly report of this series.

The manner in which the oxidations were carried out is the same as discussed in the second quarterly report. The electrolyte used was a 0.1 F potassium hydroxide solution which had been saturated with silver(I) oxide to prevent dissolution of oxide from the electrode. The reference

electrode was the mercury-mercuric oxide electrode. All the oxidations were carried out at 20 $\pm$ .01°C. The types of electrodes used were abraded foil and wire electrodes. The range of potentials was from that required just to produce silver(I) oxide on the surface of the electrode to that required to evolve oxygen at the surface of the electrode. The current and the integral of the current were recorded for all oxidations.

Potential Sweep Oxidations

These oxidations were also carried out under the same procedure as described earlier. However, instead of the potential being kept constant, it was continuously changed throughout a given oxidation. This was accomplished by replacing the constant potential reference source (D), Figure 11 of the second quarterly report, with a continuously changing potential source. A constant potential was applied across a variable ten-turn precision resistor which was rotated with a one-revolution-per-minute synchronous motor. This gave a good potential ramp source which replaced the reference potential source in the potentiostat circuit. The potential changed at a rate of 200 mv/min from 0 to 1 volt.

Constant Current Reductions

Some of the potentiostatically oxidized electrodes were reduced using constant current to determine the total charge acceptances and whether there was silver(I) or silver(II) oxide on the electrodes. The constant current reductions were carried out using the same procedures as the constant current oxidations discussed in earlier reports of this series.

Atomic Absorption

Some of the potentiostatically oxidized electrodes were stripped of the oxide film in 0.5 F ammonium hydroxide solution. The amount of

silver which had been oxidized was then determined using standard atomic absorption techniques.

RESULTS AND DISCUSSION

Charge Acceptance

The results of a comparison of the total charge acceptance as determined by (A) the current-time integral, (B) constant current reductions, and (C) amount of silver oxidized, as a function of applied potential, are given in Figure 6. While the results are inconclusive as to the relationship of each plot to the other plots, they do show the same maximum-minimum relationships. All three methods should give the same charge acceptance, at least in the potential region below 0.550 volt where only silver(I) oxide is being produced. The fact that the current-time integral is higher for all the oxidations indicates that one of three things could be happening: (1) the current efficiency may not be 100 per cent, (2) some type of auto reduction of the oxide formed may be occurring, or (3) there may still be some degree of dissolution of oxide off the surface of the electrode even though the solution is saturated in silver(I) oxide. The reason for the discrepancy between the constant current reduction plot (B) and the plot made from atomic absorption data (C) is not fully understood. Perhaps it only reflects experimental error, since some of the points are the same and one of the atomic absorption points is higher than the constant current reduction point.

The dotted line which appears in Figure 6 above 0.540 volt represents the silver(I) oxide charge acceptance as determined by the length of the silver(I) oxide reduction plateau. The solid line represents the total charge acceptance determined from the constant current reduction.

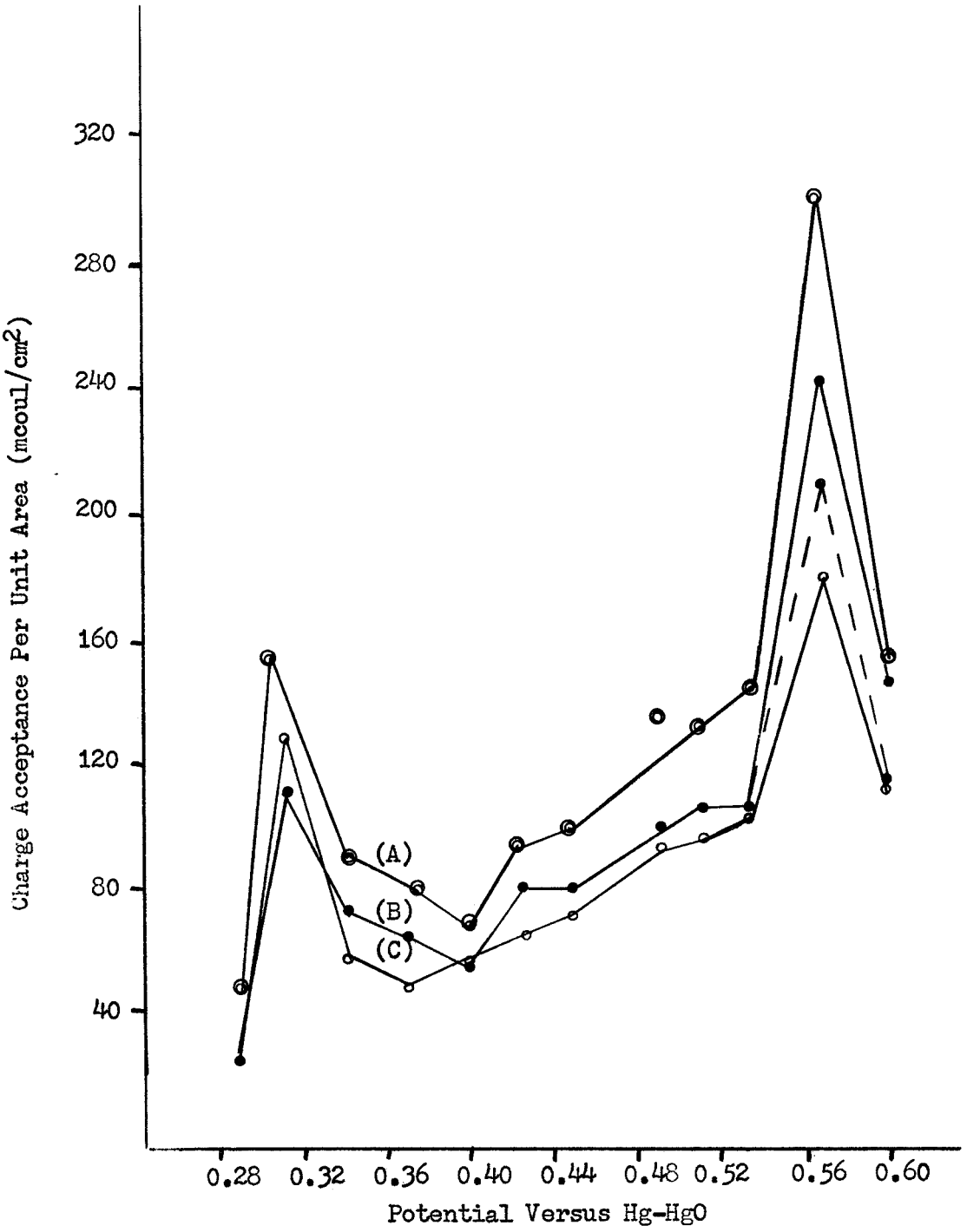

Fig. 6.--Plots of charge acceptance versus applied potential as determined by (A) current-time integral, (B) constant current reduction, (C) atomic absorption.

Potential Sweep Oxidations

The results of the potential sweep oxidations are given in Figures 7, 8, and 9. Figures 7 and 8 show the current time plots for the oxidations in saturated electrolyte of varying pH. One of the first things noted was the presence of a small initial oxidative step in addition to that of the formation of silver(I) oxide, silver(II) oxide, and oxygen. This is best shown in Figure 8 (b) as peak (a). The formation of silver(I) oxide takes place at peak (b). The formation of silver(II) oxide takes place at peak (c), and the evolution of oxygen was first noted at point (d).

Dirkse[10] reported a similar curve for a continuously changing potential of the silver electrode in alkaline solution. He suggested that the initial peak (a) was due to the formation of a silver(I) hydroxide film on the surface of the electrode. In light of Thirsk and Fleischmann's work using electron microscopy and electron diffraction techniques as well as x-ray diffraction, peak (a) is more likely the formation of the highly resistive, randomly oriented, thin film of silver(I) oxide mentioned in the introduction.

One possible approach to the determination of the nature of this initial film is to use the Flade potential-pH relationship:

$$E_f = E^o_f - 0.058\ pH.$$

The Flade potential is the potential above which an oxide surface film is formed[13].

A plot of the potential at which the initial oxide formation began versus pH is given in Figure 9. This plot was extrapolated to zero pH and a value of 0.90 volt for E^o_f versus the mercury-mercuric oxide electrode was obtained. The theoretical value for E^o_f based on the formation of an

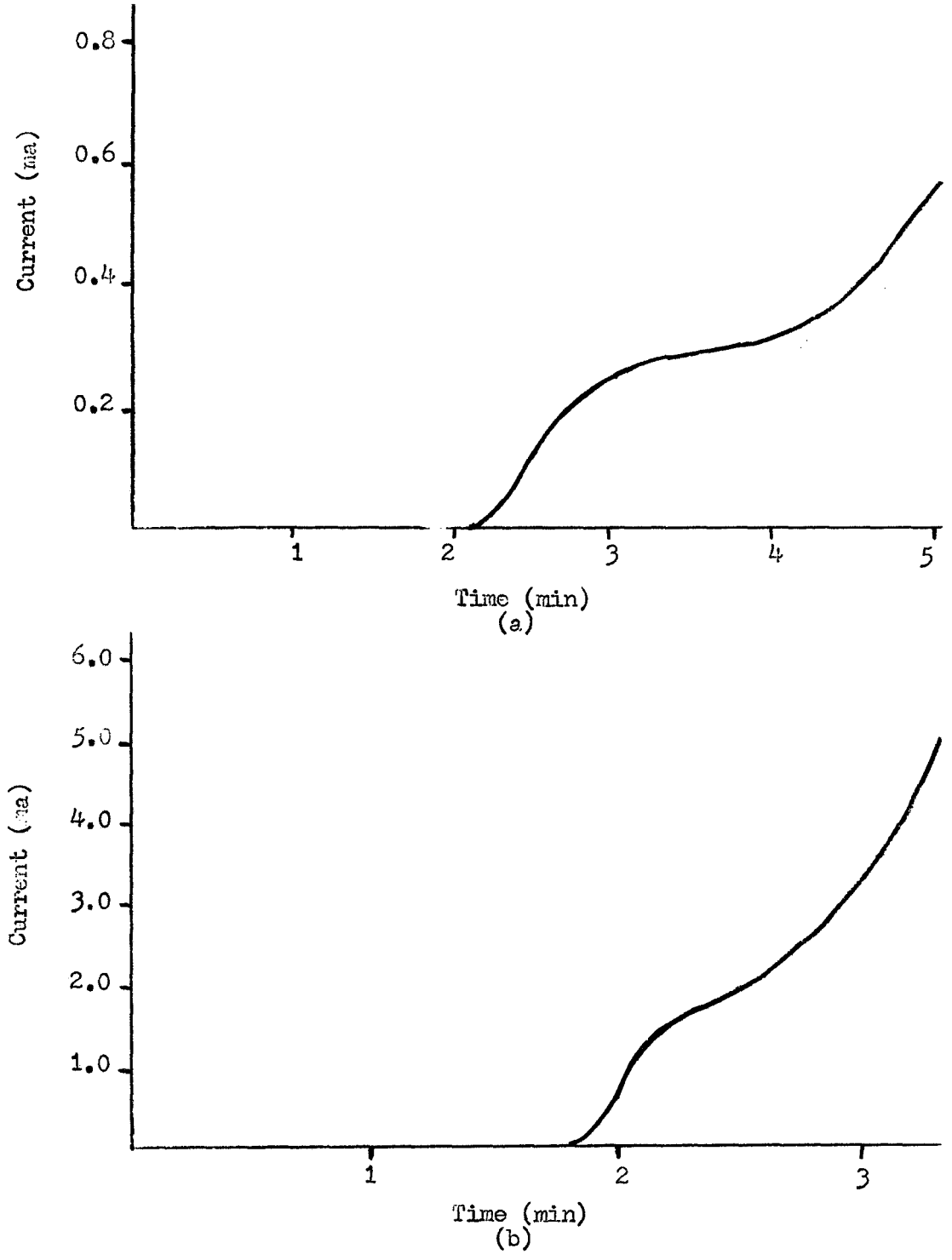

Fig. 7.--Plot of current versus time for linear potential sweep. Rate of sweep was 200 mv/min. (a) pH = 8.2 (b) pH = 10.2.

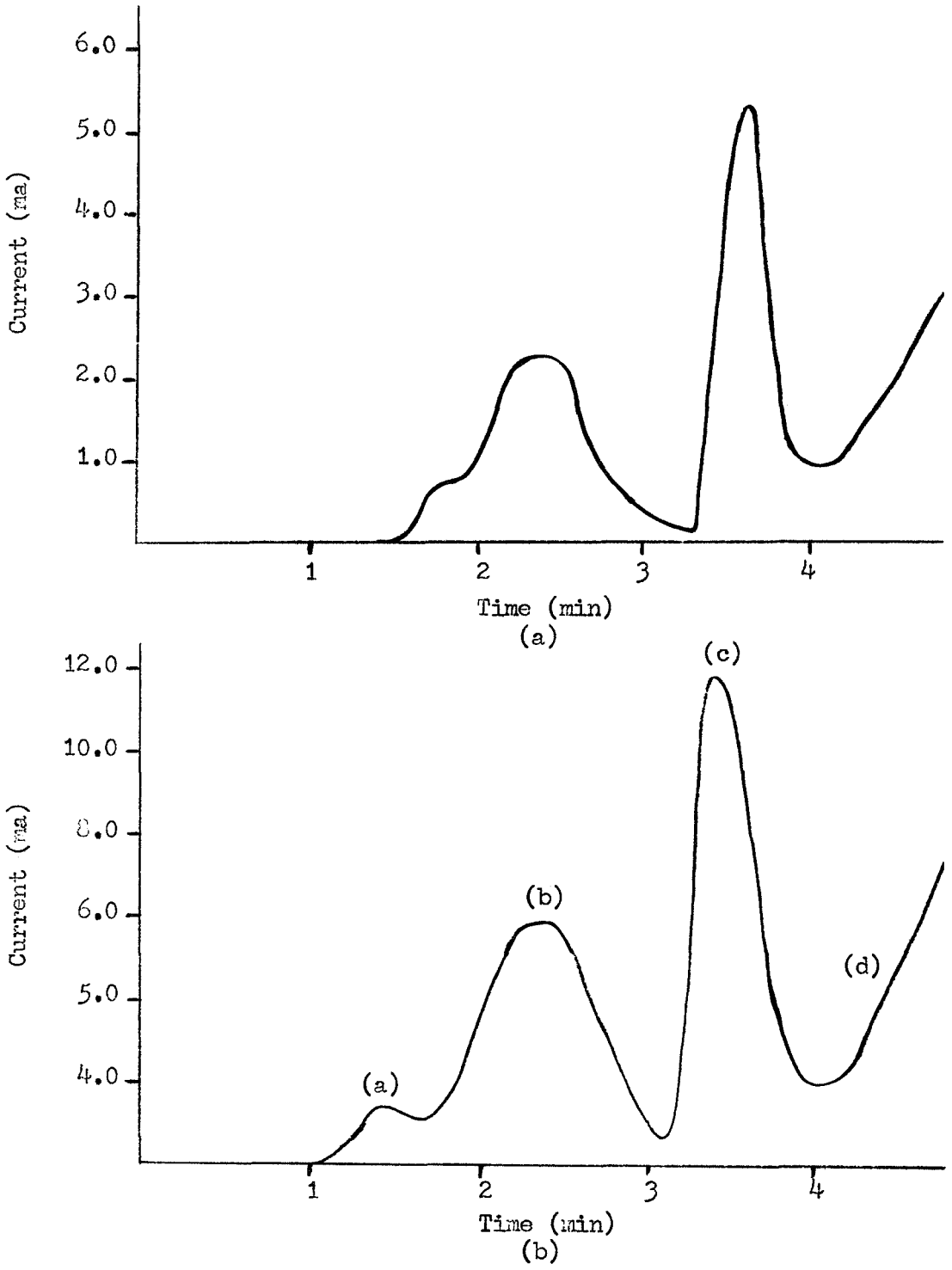

Fig. 8.--Plot of current versus time for linear potential sweep. Rate of sweep was 200 mv/min.
(a) pH = 12.5 (b) pH = 13.5.

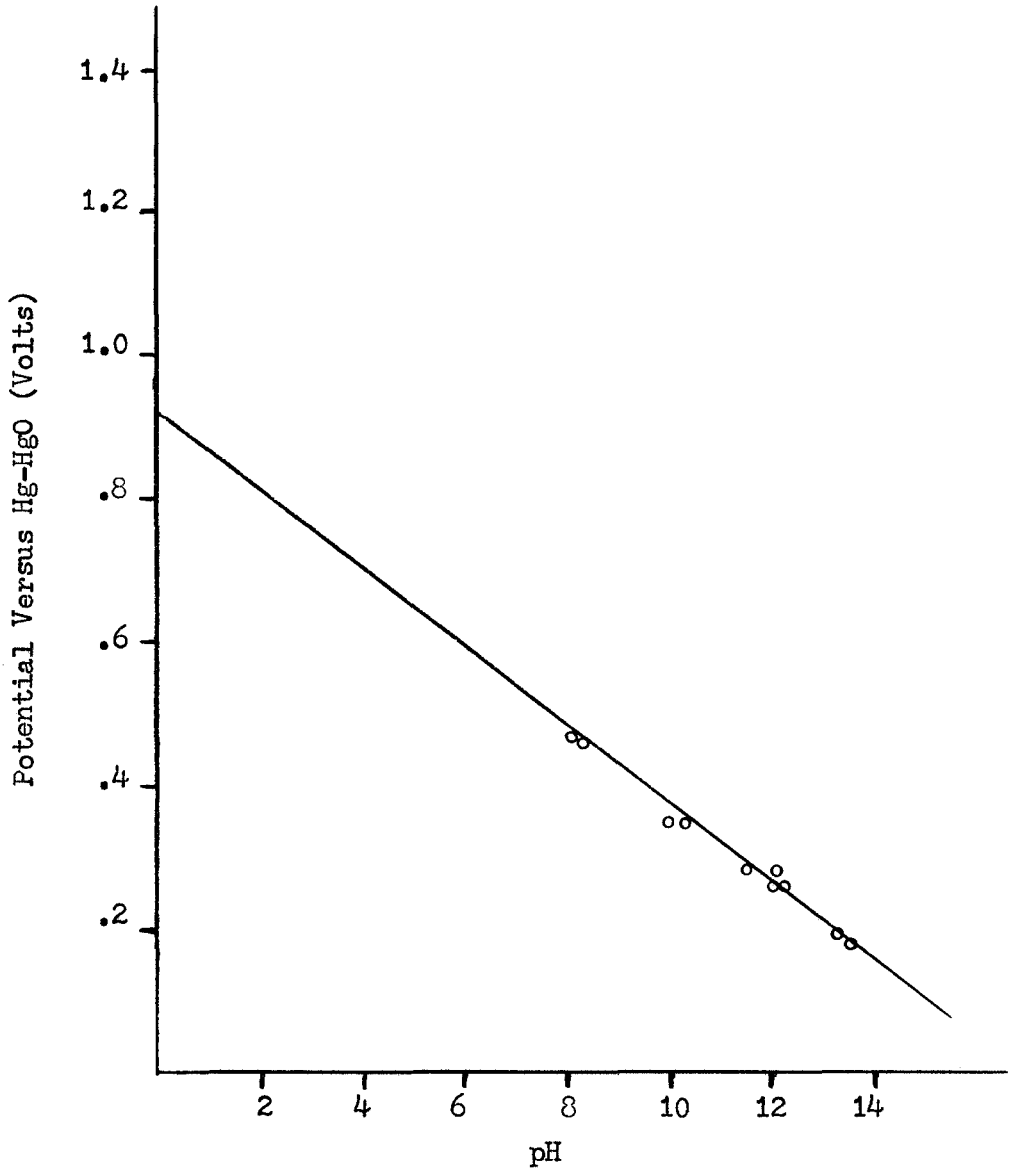

Fig. 9.--Plot of potential of initial oxide formation versus pH of saturated electrolyte.

ordered oxide is 1.28 volts versus the mercury-mercuric oxide electrode.[14] Since ΔG^{o} is proportional to E^{o}, i.e., $\Delta G^{o} = -n\ F\ E^{o}$, one can see that the free energy for the formation of the electrochemical film, at 0.90 volt, is greater than for the formation of a structured oxide, at 1.28 volts. This is reasonable, since the free energy of formation of a disordered oxide a glass for example, is greater than for the formation of the structured oxide.

Another possible interpretation which is more meaningful in terms of determining the nature and extent of the structural defects was presented by Pryor in a paper on the significance of the Flade potential.[15] He proposed a model where the gross crystallographic structure of passive film is assumed to be uniform; however, the defect concentration of passive films having thickness of the order of 100 Å will be far from uniform and will result in a marked departure from stoichiometry. Initially the nature of the defects yields an n-type semiconductor because of a considerable number of oxygen ion vacancies where electrons are trapped near the metal-oxide interface. As the film thickens, a p-type semiconductor film forms on top of the n-type. This is because of a number of metal ion vacancies creating positive holes in the lattice. The entire initial film is then a single oxide plane representing a p-n type semiconductor.

If the above model is accepted, it is clearly meaningless to attempt to calculate E^{o}_{f} in terms of free energies of formation of bulk oxide. Estimations will have to be based on the free energy of formation of energy-rich, highly defective oxide films.

At high pH values the true Flade potential is sometimes masked by the increased exchange rate between the oxide ions and the hydroxyl

ions, which gives erratic potentials spreading over as much as 400 mv.[16] The plot of potential versus pH in Figure 9 does seem to follow the predicted equation, which indicates that, in this case, the Flade potential is not masked.

Future Work

The initial thin oxide film of randomly oriented crystallites suggested by Fleischmann and Thirsk[9] will be investigated by beginning an oxidation at a potential at which small charge acceptance results. After sufficient time has elapsed to establish the basal layer of oxide, the potential will be changed to a value at which large charge acceptance is expected. If the initial basal layer determines the charge acceptance and if changing the potential does not alter the basal layer, a charge acceptance characteristic of the initial potential should result. The potential step in the opposite direction will also be investigated.

We will follow the initial current flow of potentiostatic oxidations with an oscilloscope. The physical characteristic of the recorders used previously for such studies have limited their usefulness.

S E C T I O N III

OXIDATION OF MODEL PORE ELECTRODES

Introduction

In the last Quarterly Report, preliminary work on a model pore electrode was described.[1] This work has been continued and includes: (1) modification of the electrode holder; (2) construction of model electrodes of smaller pore size; and (3) investigation of the oxidation as a function of time, wire size, and applied current.

Experimental

In the preliminary work, the electrode was constructed using 20 mil wire in a 1.5 mm diameter capillary.[1] Electrodes of smaller pore sizes have since been fabricated, using 10 mil wire in 1.5 mm capillaries and 5 mil wire in 0.7 mm capillaries. Table 2 compares several dimensions of these electrodes.

TABLE 2

DIMENSTIONS OF THREE MODEL PORE ELECTRODES

Wire diameter	20 mil	10 mil	5 mil
Capillary diameter	1.5 mm	1.5 mm	.7 mm
No. of wires	7	28	23
Ave. pore size	0.035 mm^2	.01 mm^2	0.003 mm^2
Pores per electrode	12	39	34
Surface area per mm into tube	11 mm	22 mm	9 mm

The model pore electrode shown in Figure 10 is a modification of the one shown in Figure 15a of the previous report.[1] The connecting tube (C) permits the separation of the capillary section of the holder from its complement. This results in a much shorter

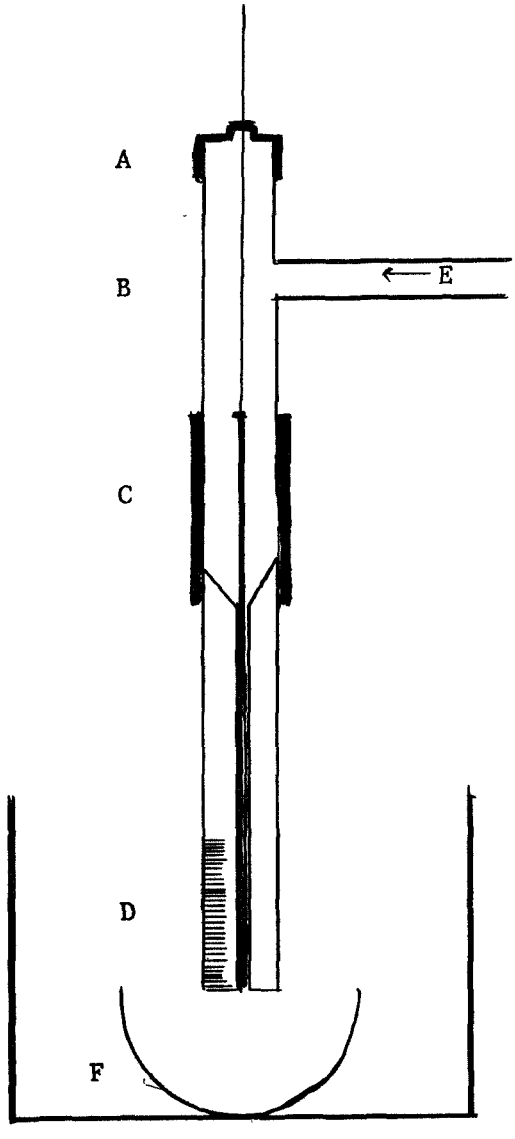

(A) Serum Cap
(B) T Joint
(C) Connecting Tube
(D) Capillary Tube
(E) Electrolyte Flow
(F) Platinum Counter Electrode

Fig. 10 Model Pore Electrode (Side View)

access distance to the capillary tube. The shorter distance simplifies the grouping of the wires and facilitates their insertion into the tube. The grouped wires were fused at the top and then connected to a 25 mil lead wire. For uniform length and parallel end surfaces, the wires were placed in the capillary so that they extended 1 mm from the end and were then sanded with 600 mesh wet and dry sandpaper. The electrode was then removed from the holder and each wire was washed with cleanser and rinsed.

The unfused ends of some of the 20 mil and 10 mil wire electrodes were masked by pressing them against a thin layer of partially cured epoxy cement. After 15 minutes the wires were individually stroked so that no cement extended beyond the edge of the tip. As before, the top of the capillary was flared, the bottom length was calibrated with marks 2 mm apart, and 0.1 F KOH solution was forced by gravity flow to pass into the arm (E), through the holder, and into the reservoir containing the counter electrode (F).

Results and Discussion

Model pore electrodes of various pore sizes were oxidized at constant currents ranging from 50 to 300 μamps. The results are shown in Table 3. They show, in general, that the extent of penetration into the pores by both silver(I) and silver(II) oxides decreases as the pore size decreases.

The results of the oxidations of the three electrodes described in Table 2 are given in Table 4. The reaction current density--i.e., the applied current divided by the surface area which is covered by Ag_2O--is approximately the same for oxidations of equal plateau length regardless of the pore size. This supports the constant current method

TABLE 3

OXIDATIONS OF MODEL PORE ELECTRODES AT VARYING APPLIED CONSTANT CURRENTS

Time (min)	Wire Size (mil)	Current (μamp)	Extent of Penetration Normal to Pore Opening: Silver(I) Oxide (mm)	Silver(II) Oxide (mm)	Oxygen
1	20	160	2.00	-	-
4	20	160	4.00	-	-
8	20	160	5.75	0.75	-
12	20	160	9.00	3.60	-
16	20	160	9.50	3.90	yes
20	20	160			
1	20	200	2.50	-	-
4	20	200	5.00	0.75	-
8	20	200	6.50	2.25	yes
1	20	240	2.50	-	-
4	20	240	5.50	2.00	yes
1	10	200	0.60	-	yes
4	10	200	2.25	-	-
8	10	200	3.80	-	-
12	10	200	4.70	1.00	-
16	10	200	6.00	1.60	-
20	10	200	6.90	2.00	-
24	10	200	7.50	2.30	-
28	10	200	8.10	2.50	yes
1	10	250	0.75	-	-
4	10	250	3.50	-	-
8	10	250	4.20	1.30	-
12	10	250	5.30	1.80	-
16	10	250	5.70	2.00	yes
1	10	300	1.50	-	-
4	10	300	3.30	0.30	-
8	10	300	4.50	1.30	yes
1	5	50	0.40	-	-
4	5	50	1.70	-	-
8	5	50	3.50	0.20	-
12	5	50	6.00	0.40	-
16	5	50	7.90	0.60	-
20	5	50	8.40	0.80	-
28	5	50	8.90	1.30	yes
1	5	75	0.70	-	-
4	5	75	3.10	-	-
8	5	75	5.00	0.50	-
12	5	75	6.30	1.20	-
16	5	75	8.40	1.60	-
28	5	75	8.70	2.00	yes

of surface area estimation that assumes that at equal plateau lengths the current densities are equal.[1]

TABLE 4

CALCULATION OF REACTION CURRENT DENSITY FROM OXIDATIONS AT CONSTANT CURRENT OF THREE MODEL PORE CAPILLARY ELECTRODES

Electrode size	20 mil	10 mil	5 mil
Surface area per mm of pore	11 mm	22 mm	9 mm
Applied current	75 μamp	200 μamp	50 μamp
Plateau length	5 min	5 min	5 min
Extent of penetration of oxidation layer into pore	2.8 mm	3.3 mm	2.0 mm
Total surface area used in reaction	30 mm^2	73 mm^2	18 mm^2
Reaction current density	2.5 $\mu amp/mm^2$	2.7 $\mu amp/mm^2$	2.7 $\mu amp/mm^2$

The effect of electrolyte flow rate was briefly studied. Difficulties encountered in controlling the flow prevent a quantitative conclusion, but it appears that both oxide films penetrate the pore to a lesser extent as the flow rate is increased. The Ag_2O film is more sensitive to this effect than is the AgO film.

Little work has been done to date on the electrodes with masked tips, but these seem to offer an excellent way to study the effects of pores, not only on the silver alkaline system, but on many other electrochemical systems. They offer controlled pore size and geometry with either stationary or forced flow electrolyte. The design also limits end effects, which is important since most theories neglect end effects in their derivations.[17, 18, 19]

References

1. E. A. Butler and A. U. Blackham, "Studies of Reaction Geometry in Oxidation and Reduction of the Alkaline Silver Electrode," Fourth Quarterly Report, J. P. L. 952268, May 15, 1969.

2. M. D. Wijnen and M. W. Smit, Recueil, 79, 289 (1960).

3. E. A. Butler and A. U. Blackham, "Studies of Reaction Geometry in Oxidation and Reduction of the Alkaline Silver Electrode," First Quarterly Report, J. P. L. 952268, August 15, 1968.

4. Ibid., Third Quarterly Report, J. P. L., 952268, February 15, 1969.

5. M. D. Wijnen and M. W. Smit, Recueil, 79, 22 (1960).

6. C. P. Wales, J. Electrochem. Soc., 117, 680 (1968).

7. M. Fleischmann and H. R. Thirsk, "Advances in Electrochemistry and Electrochemical Engineering," Vol. 3, Interscience, New York, 1963, p. 123.

8. P. A. Malachesky and R. Jasinski, Tyco Lab., Inc., Waltham, Mass.: ABS No. 174, Electrochemical Society Inc., Spring Meeting, Boston, Mass., May 5-9, 1968.

9. M. Fleischmann, P. J. Lax, H. R. Thirsk, Trans. Faraday Soc., 64, 3128 (1968).

10. T. P. Dirkse, D. B. DeVries, J. Phys. Chem., 63, 107 (1959).

11. G. T. Croft, J. Electrochem. Soc., 106, 278 (1959).

12. T. P. Dirkse, J. Electrochem. Soc., 106, 920 (1959).

13. K. J. Vetter, "Electrochemical Kinetics," Academic Press Inc., London, 1967, pp. 748-752.

14. W. M. Latimer, "Oxidation Potentials," Prentice-Hall Inc., Englewood Cliffs, Sec. Ed. (1956).

15. M. J. Pryor, J. Electrochem. Soc., 106, 557 (1959).

16. G. H. Cartledge and R. F. Sympson, J. Phys. Chem., 61, 973 (1957).

17. V. S. Daniel'-Bek, Electrokhim., 1, 1319 (1965).

18. L. G. Austin and H. Lerner, Electrochem. Acta., 9, 1469 (1964).

19. E. A. Grens and C. W. Tobias, Z. Electrochem., 68, 236 (1964).